

MIT-CTP-2839
hep-lat/9903021

The lattice Schwinger model as a discrete sum of filled Wilson loops

Christof Gattringer

Massachusetts Institute of Technology
Center for Theoretical Physics
77 Massachusetts Avenue
Cambridge MA 02139, USA

Abstract

Using techniques from hopping expansion we identically map the lattice Schwinger model with Wilson fermions to a model of oriented loops on the lattice. This is done by first computing the explicit form of the fermion determinant in the external field. Subsequent integration of the gauge fields renders a sum over all loop configurations with simple Gaussian weights depending on the number of plaquettes enclosed by the loops. In our new representation vacuum expectation values of local fermionic operators (scalars, vectors) can be computed by simply counting the loop flow through the sites (links) supporting the scalars (vectors). The strong coupling limit, possible applications of our methods to 4-D models and the introduction of a chemical potential are discussed.

To appear in Nuclear Physics B

PACS: 11.15.Ha

Key words: Lattice field theory, fermion determinant, vertex models

1 Introduction

The evaluation of the fermion determinant in lattice field theories poses a highly non-trivial problem. In particular for an odd number of flavors, or when a chemical potential is added, no fast numerical algorithms are known. As a possible way out several studies of alternative representations of the fermion determinant in terms of fermion loops can be found in the literature [1]-[10]. Loop representations are not only useful as a tool for numerical simulations, but also provide interesting insights into the nature of the fermion determinant, in particular they provide a solution of the fermion sign problem (compare [11, 12] for recent developments). At least for abelian gauge fields it is furthermore possible to perform a duality transformation for the link variables and in 2 dimensions they can even be integrated in closed form. The resulting representation in 2-D is a discrete sum over filled Wilson loops.

The historic approach to finding a loop representation for the fermion determinant is to first expand the Boltzmann factor for the fermions. Since the fermions are represented by Grassmann variables the power series for the Boltzmann factor has only finitely many terms. In a second step the Grassmann integral at each site is saturated with all possible combinations of the terms from the series for the Boltzmann factor. The result can be viewed as a sum over closed loops of links. We remark, that for gauge theories products of link variables arranged along closed loops are the only possible gauge invariant terms and thus structures of closed loops can be expected already from gauge invariance.

The local saturation of the Grassmann integral is however a tedious algebraic problem. Thus most of the results were obtained for staggered fermions where the additional structure due to spinorial degrees of freedom is avoided [1]-[5]. The resulting model however still describes more than one fermion due to the doubling problem, which is only reduced but not completely eliminated by the staggered formulation.

The first result for Wilson fermions is Salmhofer's mapping of the strongly coupled Schwinger model to a 7 vertex model [6]. The techniques used there were later generalized by Scharnhorst and applied to the strongly coupled Schwinger model with 2 flavors and the 2-D lattice Thirring model [7, 8]. Thus for purely fermionic models in 2-D also loop representations for Wilson fermions have been found for some models. However, no loop representation for the fermion determinant in an external field has been found for Wilson fermions while for the staggered case such results are known [5].

In a recent publication we have attacked this problem using a new approach [9, 10]. The central idea is to first perform a hopping expansion of the fermion determinant (see e.g. [13] for an introduction and [14] for an application to the Schwinger model). The hopping expansion essentially gives a loop representation for the free energy of fermions in an external field. Thus it already provides the natural variables for the loop representation. The remaining problem is to expand the Boltzmann factor in order to bring down the loops from the exponent. In [9, 10] this method has been applied to the case of 2-D Wilson fermions interacting with an external scalar field through a Yukawa coupling.

In this article we treat the case of the lattice Schwinger model with Wilson fermions using the hopping expansion technique. The fermion determinant in the external $U(1)$ gauge field will be written as a sum over oriented loops dressed with the gauge variables sitting on the links of the loops. In this representation we then integrate explicitly the gauge fields and the partition function turns into a discrete sum over filled Wilson loops. Vacuum expectation values of Wilson loop type observables can easily be taken into account by adding the Wilson loops to the loops from the determinant before integrating the gauge fields. VEV's of local fermionic observables (scalars and vectors) also turn out to have rather simple expressions in the loop formalism. They can be obtained by differentiating the fermion determinant (before performing the gauge field integration) with respect to the mass term for the scalars or with respect to the link variables for the vectors. In the loop picture these observables then correspond to the loop flow through sites (for the scalars) and links (vectors). Thus in a numerical simulation of the loop model the evaluation of n-point functions for these observables becomes exceedingly simple. Finally we remark, that a chemical potential can be included in a natural way by giving the pieces of loops running forward in time a weight different from the weight for pieces running backward in time.

The article is organized as follows: In the next section we rederive the hopping expansion of the fermion determinant in a form which is convenient for our later manipulations. In Section 3 we expand the Boltzmann factor and construct the loop representation of the determinant. This is done by first analyzing several examples for different contributions and subsequently the general rules of the loop calculus are discussed. In the end of Section 3 we also briefly address the role of a chemical potential. In Section 4 we discuss the relation of our new representation to known results which can

be obtained as limiting cases of our formulas. In particular the coupling to an external Yukawa field and the strongly coupled Schwinger model are considered. In Section 5 we integrate out the gauge fields and give the final representation for the partition function of the lattice Schwinger model with Wilson fermions in terms of filled loops. In Section 6 we discuss the loop representation of some observables and the article ends with a discussion in Section 7.

2 Setting and hopping expansion

We study the lattice Schwinger model with Wilson fermions. In addition to the gauge fields we also couple a real scalar field θ to the fermions through a Yukawa-type interaction. The scalar field θ will serve as a tracking device for the algebraic manipulations below and also allows for a consistency check by comparing our new representation with the known loop representation for the Yukawa-type coupling [10]. In addition we will use θ as a source term for generating n-point functions.

The Wilson lattice action is a bilinear form $S = \sum_{x,y} \bar{\psi}(x) K(x,y) \psi(y)$ with kernel

$$K(x,y) = \left[2 + m + \theta(x) \right] \delta_{x,y} - \sum_{\mu=\pm 1}^{\pm 2} \Gamma_{\mu} U_{\mu}(x) \delta_{x+\hat{\mu},y} , \quad (1)$$

where we defined

$$\Gamma_{\pm\mu} = \frac{1}{2} [1 \mp \sigma_{\mu}] \quad , \quad \mu = 1, 2 .$$

Here σ_1, σ_2 are Pauli matrices. $U_{\mu}(x) \in \text{U}(1)$ are the link variables supported on the links (x, μ) of the lattice, with $U_{-\mu}(x) = U_{\mu}(x - \hat{\mu})^*$, ($\mu = 1, 2$), i.e. for hopping in backward direction the link variables are complex conjugate. The sum in the bilinear form runs over the whole lattice, $x, y \in \Lambda$. For simplicity we assume that our lattice Λ is a finite rectangular piece of \mathbb{Z}^2 with open boundary conditions, i.e. hopping terms that would lead to the outside of our lattice are omitted. We remark that all our results also hold for Λ being a cylinder with a compact time direction with anti-periodic boundary conditions and open boundary conditions for the space direction. Such a geometry is interesting for analyzing the model at finite temperature. Let's define

$$M(x) = 2 + m + \theta(x) ,$$

and assume that $\theta(x)$ is such that $M(x) \neq 0$ for all lattice points x . This is a purely technical assumption due to the particular techniques we use for computing the determinant. The final result will be a finite polynomial in the $\theta(x)$ and the above restriction is irrelevant then. We now can write for the fermion determinant

$$\begin{aligned} & \int d\bar{\psi} d\psi \exp \left(- \sum_{x,y \in \Lambda} \bar{\psi}(x) K(x,y) \psi(y) \right) = \det K \\ &= \prod_{x \in \Lambda} M(x)^2 \det(1 - H) = \prod_{x \in \Lambda} M(x)^2 \exp \left(- \sum_{n=1}^{\infty} \frac{1}{n} \text{Tr } H^n \right). \quad (2) \end{aligned}$$

In the last step the hopping expansion was performed, i.e. the determinant was expressed using the well known trace-logarithm formula and the logarithm was expanded in a power series. The hopping matrix H is defined as

$$H(x, y) = \sum_{\mu=\pm 1}^{\pm 2} \Gamma_{\mu} \frac{U_{\mu}(x)}{M(x)} \delta_{x+\hat{\mu}, y}. \quad (3)$$

The series in the exponent of (2) converges for $\|H\| < 1$, and the whole expression represents the determinant then (see e.g. [15]). In [16] it is shown for the case of $\theta(x) = 0$, that $\|H\| < 1$ for $m > 0$. It is straightforward to generalize this argument and prove that for our case we have $\|H\| < 1$ for $m + \theta(x) > 0$. To summarize: the series in (2) converges for $m + \theta(x) > 0$ and the right hand side of (2) represents the determinant for this range of parameters.

Due to the Kronecker delta in (3), the contributions to $\text{Tr } H^n$ are supported on closed loops on the lattice, and since closed loops are of even length (for the cylinder geometry discussed above we assume an even length for the compact direction), the contributions for odd n vanish. For even $n = 2k$ we obtain

$$\text{Tr } H^{2k} = \sum_{x \in \Lambda} \sum_{l \in \mathcal{L}_x^{(2k)}} \prod_{(y, \mu) \in l} \frac{U_{\mu}(y)}{M(y)} \text{Tr} \prod_{\nu \in l} \Gamma_{\nu}. \quad (4)$$

Here $\mathcal{L}_x^{(2k)}$ is the set of all closed, connected loops of length $2k$ and base point x . In the first product we collect all the link variables $U_{\mu}(y)/M(y)$ on the links visited by the loop according to their orientation. The last term in (4) is the trace of the ordered product of the hopping generators Γ_{ν} as they appear along the loop l . We remark, that $\Gamma_{\pm\nu}\Gamma_{\mp\nu} = 0$, which implies that

whenever a loop turns around at a site and runs back along its last link this contribution vanishes. Thus all these *back-tracking* loops can be excluded from $\mathcal{L}_x^{(2k)}$.

Evaluating the trace over the matrices Γ_ν for a given loop is the remaining problem in the hopping expansion. It first has been solved for the infinite lattice in [17] by realizing that the Pauli matrices give rise to a representation of discrete rotations on the lattice. Alternatively one can build up the loops using four basic steps and compute the trace in an inductive procedure along the lines of [18]. The latter method can be extended to the case of lattices with compact dimensions. When choosing a cylinder with anti-periodic boundary conditions in time direction and open b.c. for the space direction the result equals the result for the rectangular lattice with open boundary conditions. Thus the result for both of the discussed sets of boundary conditions is

$$\text{Tr} \prod_{\nu \in l} \Gamma_\nu = -(-1)^{s(l)} \left(\frac{1}{\sqrt{2}} \right)^{c(l)}. \quad (5)$$

By $s(l)$ we denote the number of self-intersections of the loop l and $c(l)$ gives its number of corners. We remark, that for e.g. a torus additional sign factors for topologically non-trivial loops would appear. The result (5) is independent of the orientation of the loop. Inserting (4) and (5) in (2) we obtain

$$\begin{aligned} \det K &= \prod_{x \in \Lambda} M(x)^2 \exp \left(\sum_{k=1}^{\infty} \frac{1}{2k} \sum_{y \in \Lambda} \sum_{l \in \mathcal{L}_y^{(2k)}} (-1)^{s(l)} \left(\frac{1}{\sqrt{2}} \right)^{c(l)} \prod_{(z, \mu) \in l} \frac{U_\mu(z)}{M(z)} \right) \\ &= \prod_{x \in \Lambda} M(x)^2 \exp \left(\sum_{l \in \mathcal{L}} \frac{(-1)^{s(l)}}{I(l)} \left(\frac{1}{\sqrt{2}} \right)^{c(l)} \prod_{(y, \mu) \in l} \frac{U_\mu(y)}{M(y)} \right). \end{aligned} \quad (6)$$

In the second step we removed the explicit summation over the base points. A loop of length $2k$ without complete iteration of its contour allows for $2k$ different choices of a base point thus canceling the factor $1/2k$ in the previous expression. A loop which iterates its whole contour $I(l) > 1$ times allows only for $2k/I(l)$ different base points and a factor $1/I(l)$ remains (compare [17, 18] for a more detailed discussion). We defined \mathcal{L} to be the set of all closed, connected, non back-tracking loops of arbitrary length. Note that each loop comes with both of its orientations and the factors from the link variables for the two orientations are complex conjugate to each other.

3 Expansion of the Boltzmann factor and identification of the loop representation

The final expression (6) for the hopping expansion performed in the last section is the starting point for the identification of the loop representation for the determinant in this section. As already outlined in the discussion above we will proceed by expanding the Boltzmann factor. This expansion converges and represents the determinant when the sum in the exponent converges, i.e. for $m + \theta(x) > 0$ as discussed above. The resulting series converges even absolutely and the reordering of terms which we perform below is justified (see e.g. [19]).

We approach the expansion by first discussing several examples which will be used to extract the general algebraic rules for the different terms along the way. Keeping track of the terms in the Taylor expansion of the Boltzmann factor is most easily done by using the actual contours of the loops associated with the different terms. So let's first look at the different contributions to the sum in the exponent of the Boltzmann factor. In Fig. 1 we show some of the terms as they appear in the exponent.

The first two terms are two loops around a single plaquette and they differ only in their orientation. Note that each of these two loops (similarly for all loops shown) is only a representative for all loops around a single plaquette, the other loops differing by a translation, i.e. winding around any other single plaquette of the lattice. These first two loops both have four corners thus giving rise to a geometrical factor of $(1/\sqrt{2})^4$. Certainly there are also the factors from taking the product of the link variables around the plaquette. These are however not relevant for the following discussion and thus are not displayed explicitly. We show only the corner-, self-intersection- and iteration-factors.

Next we plot another rectangular loop, but now enclosing six plaquettes. Again the corner-factor is $(1/\sqrt{2})^4$. The fourth term is a loop enclosing two plaquettes but now having a pinch structure. This loop has eight corners and no self-intersection such that its geometrical weight is $(1/\sqrt{2})^8$. The next term we show is again a loop enclosing the same two plaquettes, the lower plaquette however is now run through with opposite orientation. This loop has one self-intersection, but only 6 corners, thus producing a factor of $-(1/\sqrt{2})^6$. Note that also the weight from the link variables (not displayed in Fig. 1) differs from the last contribution since the lower plaquette now has negative orientation and the link variables for this plaquette are complex

$$\begin{aligned}
\text{Boltzmann factor} = \exp & \left(\left(\frac{1}{\sqrt{2}}\right)^4 \begin{array}{c} \leftarrow \rightarrow \\ \rightarrow \leftarrow \end{array} + \left(\frac{1}{\sqrt{2}}\right)^4 \begin{array}{c} \rightarrow \leftarrow \\ \leftarrow \rightarrow \end{array} + \dots \\
& + \left(\frac{1}{\sqrt{2}}\right)^4 \begin{array}{c} \rightarrow \rightarrow \rightarrow \rightarrow \\ \leftarrow \leftarrow \leftarrow \leftarrow \end{array} + \dots + \left(\frac{1}{\sqrt{2}}\right)^8 \begin{array}{c} \leftarrow \rightarrow \\ \rightarrow \leftarrow \\ \leftarrow \rightarrow \\ \rightarrow \leftarrow \end{array} + \dots \\
& - \left(\frac{1}{\sqrt{2}}\right)^6 \begin{array}{c} \leftarrow \rightarrow \\ \rightarrow \leftarrow \\ \leftarrow \rightarrow \\ \rightarrow \leftarrow \end{array} + \dots - \frac{1}{2} \left(\frac{1}{\sqrt{2}}\right)^8 \begin{array}{c} \leftarrow \rightarrow \\ \rightarrow \leftarrow \\ \leftarrow \rightarrow \\ \rightarrow \leftarrow \end{array} + \dots \\
& - \left(\frac{1}{\sqrt{2}}\right)^8 \begin{array}{c} \rightarrow \rightarrow \rightarrow \rightarrow \\ \leftarrow \leftarrow \leftarrow \leftarrow \end{array} + \dots \left. \vphantom{\exp} \right)
\end{aligned}$$

Figure 1: *Graphical representation for some of the terms in the exponent of the Boltzmann factor. We display only the corner-, self-intersection- and iteration-factors.*

conjugate. Next we show a loop which runs around a single plaquette twice. It has eight corners and one self intersection. In addition we have to take into account a factor of $1/2$ since the loop iterates its contour twice. The total factor then is $-1/2(1/\sqrt{2})^8$. Finally we show another loop with a self-intersection. It consists of 2 loops around single plaquettes connected by a double line along two links. It has one self-intersection and 8 corners such that the geometrical factor is $-(1/\sqrt{2})^8$.

Note that in Fig. 1 we display only a few terms which are useful for the discussion of some examples below. It is however straightforward to depict arbitrary terms from the series in the exponent of (6) and to determine the corresponding geometrical factors.

Let's now perform the expansion of the Boltzmann factor in (6). We will proceed as follows: In the figures below we show on the left hand side some configuration of links as it appears in the final representation, i.e. after the Boltzmann factor has been expanded. These contributions in their

final form will however be built from different loops and their products, emerging when expanding the Boltzmann factor. These different terms are shown in the middle of the figures below, together with their geometrical weights. The total weight associated to the graph depicted on the left hand side is the sum of the weights for all contributing terms. We give this number on the right hand side, separated by an arrow. We remark that the expansion of the Boltzmann factor will produce contributions consisting of several disconnected pieces located on different positions of our lattice. Up to the combinatorial factors which will be discussed below, disconnected pieces in different areas of the lattice do not communicate with each other. Our examples thus concentrate on the different terms locally building up a contribution. The inclusion of disconnected pieces located elsewhere is a trivial generalization.

$$\text{Loop} \sim \left(\frac{1}{\sqrt{2}}\right)^4 \text{Loop} \longrightarrow \left(\frac{1}{\sqrt{2}}\right)^4$$

Figure 2: *A loop around a single plaquette.*

In Fig. 2 we show a loop which consists only of the four links around a single plaquette. As is obvious from Eq. (6) and its geometrical representation in Fig. 1, there is only one contribution in the Taylor expansion of the Boltzmann factor giving rise to this contribution. It is the first loop depicted in Fig. 1. Furthermore only the linear term in the power series for the exponential function produces this term since for higher powers, this loop would be multiplied with other loops. Thus we find only one term on the right hand side of Fig. 2. The total weight for this term is the same as we had in the exponent, namely $(1/\sqrt{2})^4$.

$$\text{Loop} \sim -\frac{1}{2} \left(\frac{1}{\sqrt{2}}\right)^8 \text{Loop} + \frac{1}{2} \left(\frac{1}{\sqrt{2}}\right)^8 \text{Loop} \times \text{Loop} \longrightarrow 0$$

Figure 3: *A loop which iterates its contour twice.*

Next we consider a contribution where a loop iterates its contour twice (Fig. 3). In particular we consider the simplest such term, i.e. the configuration where all links around a simple plaquette are occupied twice. This configuration firstly can be resolved with a single connected loop. This loop

has eight corners and one self-intersection which produces a minus sign. In addition we have to take into account a factor of $1/2$ since this loop completely iterates its contour twice. The overall factor thus is $-1/2(1/\sqrt{2})^8$. Secondly the configuration can be resolved as the square of the loop which runs around our plaquette only once. Each of the single loops has four corners giving a total corner factor of $(1/\sqrt{2})^8$. In addition one has a factor $1/2$ which is the factor for the quadratic term in the power series of the exponential function. Putting things together we find that the two contributions cancel each other.

This type of cancellation which we have seen in the simple example of Fig. 3 is the manifestation of a general rule: Whenever a term contains a loop which iterates its complete contour twice the contribution gets canceled. The general argument goes as follows: Let l_1 be the loop which iterates its contour twice. Assume, that it appears in a contribution which also contains $n - 1$ other loops $l_i, i = 2, \dots, n$, which are located somewhere else on the lattice. This contribution then appears in the n -th power term of the Taylor series for the exponential function. The corresponding factor is:

$$\frac{1}{n!} \frac{-1}{2} \left(\frac{1}{\sqrt{2}} \right)^{c(l_1)} f(l_2) f(l_3) \dots f(l_n) n! . \quad (7)$$

The $1/n!$ factor on the left hand side comes from the power series for the exponential function. Then follows a minus sign from the self-intersection of l_1 and a factor of $1/2$ since l_1 iterates its contour twice. Next we have the corner factor for l_1 followed by the factors $f(l_i)$ for the other loops (corner, self-intersection- and iteration-factors). Finally we find a combinatorial factor of $n!$ which gives the number of different ways the n terms can be arranged. Since l_1 iterates its contour twice, the same contribution can also be obtained by squaring a loop l'_1 which has the same contour as l_1 , but runs through it only once. This contribution then appears in the $n + 1$ -th power term of the Taylor series for the exponential function and comes with a factor of

$$\frac{1}{(n+1)!} \left(\frac{1}{\sqrt{2}} \right)^{c(l_1)} f(l_2) f(l_3) \dots f(l_n) \frac{(n+1)!}{2} . \quad (8)$$

Here the factor of $-1/2$ is gone, since we have no self-intersection and also the contour is not run through twice by a single loop. The corner factor stays the same since $c(l_1) = 2c(l'_1)$. Finally the combinatorial factor changes to $(n+1)!/2$, where the factorial gives the number of ways the $n+1$ terms can be arranged. However, l'_1 appears twice, such that we have to divide by 2. Thus we find that (7) is exactly the negative of (8). This proves

that whenever a loop iterates its contour twice it can be matched with a contribution which has the opposite sign and gets canceled.

In principle one can extend this proof and show via induction that all contributions, where a loop completely iterates its contour more than once, get canceled. There is however a simpler argument. It is based on the fact, that not more than two lines can flow through a site. To understand this we have to remember that each occupied link carries with it a factor of $1/M(x)$ as can be seen from the last product in (6). Thus when n loops run through a site x_0 they produce a factor of $1/M(x_0)^n$. Combined with the overall factor of $M(x_0)^2$ we find $M(x_0)^{2-n}$. When n exceeds 2, i.e. more than two loops run through a site, this term is no longer polynomial. On the other hand one finds by direct evaluation that the expression for the determinant on the finite lattice is a polynomial in $M(x_0)$. Using the fact that for $m + \theta(x) > 0$ the series represents the determinant (compare the discussion above) we conclude, that all vertices where more than 2 lines run through a site have to vanish. This implies that loops which iterate their contour more than twice cannot contribute and for the case of the doubly iterated loop we have given the explicit argument for its cancellation above, thus showing that eventually none of the iterating loops in the exponent contributes.

Before we go back to the discussion of further examples, let's bring in another harvest from the discussion in the last few paragraphs: The factors $1/n!$ from the Taylor series of the exponential function always get canceled and the combinatorial factor simply is 1. This can be seen as follows: For a contribution which is the product of n loops one finds that only terms where n different loops are multiplied can contribute (if a loop could appear more than once we would have loops which are multiply occupied, a case which we have just excluded). These products come with a combinatorial factor of $n!$, which gives the number of ways the terms can be arranged. It cancels the factor of $1/n!$ from the Taylor series for the exponential function. Thus the algebraic factor is always equal to 1.

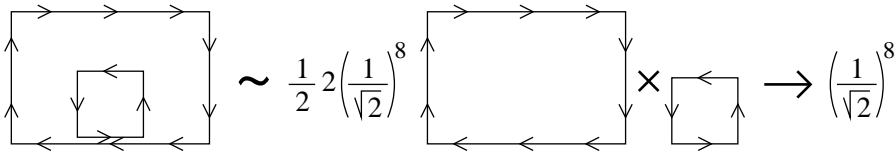


Figure 4: Two nested loops with opposite orientation.

After this combinatorial excursion let's go back to discussing more examples. Next we analyze a graph with two nested loops (Fig. 4). There is only one contribution in the expansion of the Boltzmann factor giving rise to this graph. It is a product of two loops, i.e. it comes from the quadratic term in the Taylor series for the exponential function. Thus it has a factor of $1/2$ which is the coefficient of the quadratic term in the Taylor series. However, for our graph two different loops have to be multiplied, making our contribution a cross term which comes with a factor of 2 canceling the factor $1/2$ from the power series. Each of the two loops has 4 corners giving rise to a geometrical factor of $(1/\sqrt{2})^8$. This is already the final factor associated with the contribution depicted on the left hand side of Fig. 4.

$$\begin{aligned}
& \text{Diagram of two nested loops with equal orientation} \sim - \left(\frac{1}{\sqrt{2}}\right)^8 \text{Diagram of two separate loops} \\
& + \frac{1}{2} 2 \left(\frac{1}{\sqrt{2}}\right)^8 \text{Diagram of a large loop} \times \text{Diagram of a small loop} \rightarrow 0
\end{aligned}$$

Figure 5: *Two nested loops with equal orientation.*

In Fig. 5 we look at a graph which contains the same links, but the orientation of the inner loop has been reversed. In addition to the contribution from a product of two loops, similar to the last example, the new configuration also allows for a single connected loop running through the chosen set of links. This term is produced by the linear term of the power series for the exponential function and thus simply has an algebraic factor of 1. The geometric factor is $-(1/\sqrt{2})^8$, since the loop has eight corners and one self-intersection. The product contribution has the same factor as in the last example. The two contributions cancel each other.

Fig. 5 demonstrates another general rule of our loop calculus: The final expression will not contain any terms where a link is occupied twice with the same orientation. Whenever we compute the weight for such a graph we find that the different terms in the expansion of the Boltzmann factor cancel each other. In Fig. 5 this is demonstrated in an example, but let's give the general argument: Whenever we have a configuration where along at least

one link two lines run parallel with the same orientation, then there are two ways to resolve this configuration with terms coming from the expansion of the Boltzmann factor. One contribution where the two lines do not cross and one with a crossing. Both contributions have the same number of corners, the latter one however obtains an extra minus sign due to the additional self intersection. The two terms thus cancel each other. We remark that at some other parts of our loop there also might be structures which can be resolved in different ways. However, already one link which is run through twice in the same direction leads to a vanishing of this contribution (compare also the discussion of completely iterated loops given above). This exclusion of contributions with links which are run through twice in the same direction can be interpreted as a manifestation of the Pauli principle which forbids two excitations of the same state.

$$\text{Diagram of a self-intersecting loop} \sim \left(\frac{1}{\sqrt{2}}\right)^8 \text{Diagram of a single loop with 8 corners} + \frac{1}{2} 2 \left(\frac{1}{\sqrt{2}}\right)^8 \text{Diagram of two separate loops} \rightarrow \left(\frac{1}{\sqrt{2}}\right)^6 \text{Diagram of a loop with 6 corners}$$

Figure 6: A configuration with a self intersection.

Next we concentrate on how a configuration containing an intersection can be resolved in different ways. The left hand side of Fig. 6 shows a configuration which contains two plaquettes with opposite orientation which share a common corner. There is one possibility to run around the two plaquettes in a single loop. This contribution comes from the linear term in the Taylor series for the exponential function and has eight corners thus acquiring a factor of $(1/\sqrt{2})^8$. Our two plaquettes can also be obtained as the product of two loops, i.e. a contribution appearing in the quadratic term of the power series. Again we have a total of eight corners giving a factor of $(1/\sqrt{2})^8$ and when adding this to the coefficient of the linear term we find an overall factor of $(1/\sqrt{2})^6$.

In the configuration shown in Fig. 7 we now have reverted the orientation of the lower plaquette. Certainly this configuration will still have a contribution from the quadratic term of the exponential function where it is written as a product of two loops. The geometrical factor is the same as in the last example. However, the linear term, where our contour appears as a single connected loop, has to be changed. It now has only six corners but one self-intersection and thus a factor of $-(1/\sqrt{2})^6$. Adding this to the

$$\sim -\left(\frac{1}{\sqrt{2}}\right)^6 + \frac{1}{2} 2 \left(\frac{1}{\sqrt{2}}\right)^8 \rightarrow -\left(\frac{1}{\sqrt{2}}\right)^8$$

Figure 7: *Another configuration with a self intersection.*

coefficient of the product term we find an overall factor of $-(1/\sqrt{2})^8$.

$$\sim -\left(\frac{1}{\sqrt{2}}\right)^8 \rightarrow -\left(\frac{1}{\sqrt{2}}\right)^8$$

Figure 8: *Loops around two plaquettes joined by a double line.*

Finally we discuss (Fig. 8) the contribution which corresponds to the last loop shown in Fig. 1. It cannot be decomposed into the product of two loops and thus is entirely built from the linear term in the expansion of the exponential function. The factor $-(1/\sqrt{2})^8$ is simply taken over from the exponent. Although not very interesting from a combinatorial point of view, this example demonstrates another important point. In order to avoid overcounting of self-intersections, we have to introduce a normal ordering for double lines with two flows in opposite direction (the case of lines with equal direction has already been ruled out above). We always draw a line that flows from left to right above a line which flows from right to left. For vertical double lines we adopt the convention that downward flowing lines are drawn on the right hand side of upward flowing lines.

After having analyzed several of these examples one finds that the contributions on the left hand side can be decomposed into finitely many elements and all contributions which appear in the expansion of the Boltzmann factor can be built from these elements. We view these elements as tiles with some configurations of oriented lines drawn on these tiles (compare Fig. 9). The tiles can now be arranged on our rectangular lattice such that ingoing and outgoing flow lines on neighboring tiles match each other. To each tile we assign a weight w_i and the total weight of a configuration is given by the product of all weights for the tiles which were used in building the configuration. When summing over all possible ways of different tilings of

our lattice (placing the centers of the tiles on the sites of the lattice) we reproduce all possible fermion loops contributing to the fermion determinant. The concept of writing partition functions as a sum over tiles (vertices) was first introduced in [20, 21] and these models are known as vertex models (see also [22]).

The remaining problem is to assign the correct weights to our tiles. From the example shown in Fig. 2 we find that a simple corner has to be assigned a factor of $1/\sqrt{2}$ which gives the weights w_5, \dots, w_{12} in Fig. 9. Fig. 4 shows that tiles with a straight line (w_1, \dots, w_4 in Fig. 9) obtain a factor of 1. The same factor has to be assigned when two straight lines run anti-parallel (w_{44}, w_{45}). The example discussed in Fig. 8 furthermore shows that antiparallel flow lines have to be normal ordered and our convention is to draw flow lines from left to right above flows from right to left and downward flows are drawn right of upward lines. From Fig. 4 we learn, that tiles with a straight line and a corner (w_{19}, \dots, w_{34} in Fig. 9) have a factor of $1/\sqrt{2}$ and an additional minus sign if the normal ordering of the double line enforces a crossing. Similarly one finds that tiles with two corners ($w_{35}, \dots, w_{42}, w_{46}, \dots, w_{49}$ in Fig. 9) have a factor of $(1/\sqrt{2})^2 = 1/2$, again with an additional minus sign if a crossing occurs. Figs. 3,5 and the general argument given there establish that all tiles which contain two lines running parallel in the same direction must have vanishing weights (these tiles are not displayed in Fig. 9). From Figs. 6,7 we find that for tiles showing two crossing lines we have to assign a factor of $-1/2$ when the crossing can be resolved with a self-intersecting loop (w_{13}, \dots, w_{16}) and a factor of 1 when no self-intersecting resolution is possible (w_{17}, w_{18}). Finally we also have to include the empty tile (w_{43}) which has a factor of 1. In Fig. 9 we give a complete list of all 49 tiles with non-vanishing weights.

We remark that tiles with an odd number of incoming or outgoing lines of flow cannot appear, since all contributions come from products of closed loops and thus the net flow into a site has to vanish. Furthermore not more than two lines can run through a vertex as follows from the fact that the determinant is a polynomial in the local mass terms (see the discussion below Eq. (8)). The final expression for the fermion determinant reads

$$\det K = \prod_{x \in \Lambda} M(x)^2 \sum_{t \in \mathcal{T}} \prod_{j=1}^{49} (w_j)^{n_j(t)} \prod_{(y, \mu) \in t} \frac{U_\mu(y)}{M(y)}. \quad (9)$$

Here we introduced the set \mathcal{T} of all admissible tilings of our lattice Λ with the tiles depicted in Fig. 9, i.e. the set of all arrangements of tiles such that

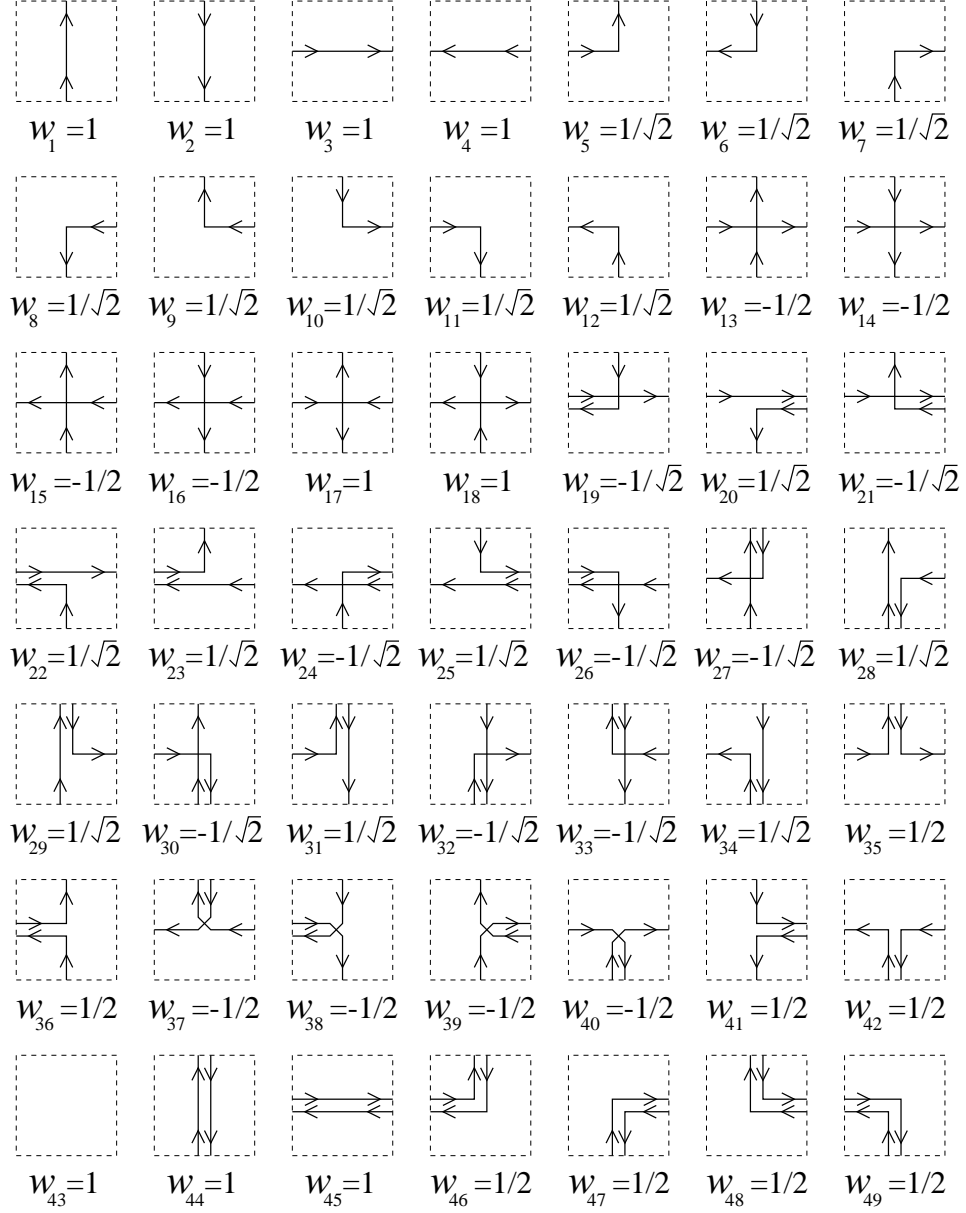


Figure 9: The 49 tiles (vertices) with non-vanishing weights w_i .

the flow lines on neighboring tiles match. By $n_j(t)$ we denote the abundance of tile number j in a particular tiling $t \in \mathcal{T}$. The last product runs over all links occupied by the tiling t . For links run through in negative direction, the link variables have to be complex conjugated. Our result is valid for two sets of boundary conditions: 1.) The fermions have open boundary conditions for both directions. In this case also the vertex model has open boundary conditions for both directions. 2.) The fermions have one direction with open boundary conditions and the second direction is compactified with anti-periodic boundary conditions for the fermions (cylinder geometry). The vertex model then has open boundary conditions for one direction, whereas the boundary conditions for the compact direction are periodic.

Let's now briefly discuss the applicability of our method to higher dimensional theories and non-abelian gauge groups. The first step will again be a hopping expansion leading to formula (2). As in two dimensions this series will converge and represent the determinant for $\|H\| < 1$. Along the lines of the proof in [16] one can again establish this bound on the norm of the hopping matrix for a certain range of values for the mass m and the auxiliary field θ . Also the trace over the gamma matrices is known in four dimensions [17]. For the parameters where $\|H\| < 1$ the Boltzmann factor can be expanded in the same way as in 2-d, and the resulting series represents the determinant [15]. Again we can apply the power counting trick for the local mass terms and show, that the number of fermion lines admissible at a single site is bounded. In four dimensions this bound is given by $4N_c$ where N_c denotes the number of colors. For non-abelian gauge fields in addition one has to take the trace over the product of the link variables. The resulting formula is the loop representation of the fermion determinant.

Such loop representations can be seen to lead to new ways for a numerical evaluation of the fermion determinant by directly updating the loop configurations [23]. It is now possible to overcome the limitations of pseudo-fermion methods and simulate also odd numbers of flavors. For e.g the one-flavor lattice Schwinger model with Wilson fermions no numerical analysis exists and we are currently implementing algorithms based on the loop representation for this model [23].

In this context it is interesting to note, that the loop representation for the fermion determinant also solves the fermion sign problem. This problem plagues a direct evaluation of the Grassmann path integral [11], as well as the Hamiltonian treatment of fermionic systems [12]. When numeri-

cally updating fermions, the fermion sign problem enforces an exponentially increasing number of Monte-Carlo configurations as the volume of the system is increased or its temperature is lowered [12]. In our representation these permutation signs are gone and the remaining signs are due to the traces over the gamma matrices. These latter signs are less severe, since the weights for configurations with negative sign are exponentially suppressed due to additional factors of $1/\sqrt{2}$ which are necessary to build loops with self intersections.

Finally we argue that the loop representation could also lead to new methods for the simulation of lattice field theories with non-vanishing chemical potential. Although the Schwinger model with chemical potential is not particularly interesting per se (see e.g. [24] for a study in the continuum) it nevertheless poses the same technical problems as QCD with chemical potential. When introducing the chemical potential μ along the lines of [25] each link forward in time obtains a factor of $e^{-\mu}$ and a factor of $e^{+\mu}$ for links backward in time. Thus the symmetry between the two possible orientations of loops winding around the compact direction is broken and the determinant acquires a complex phase. This complex phase prohibits the application of the pseudo-fermion method which requires a non-negative kernel for the action of the pseudo-fermions. The loop representation allows for an update of single loops and the chemical potential can be included in a natural way independent of the number of dimensions. Also this idea is currently being tested [23] using Thirring- and Gross-Neveu-type models in loop representation.

4 Two limiting cases of our representation

Our final representation (9) of the fermion determinant has a relatively simple form. It is however instructive to reduce it to limiting cases and compare it to known results for these instances which were obtained with different methods. In particular we will discuss the case of the determinant in a scalar background field and the case of the strongly coupled Schwinger model.

We start with the case of the reduction to the case of the fermion determinant in a scalar background field [9, 10]. There the result for the fermion

determinant reads

$$\det K = \prod_{x \in \Lambda} M(x)^2 \left(\sum_{l \in \mathcal{L}_{sa}} \left(\frac{1}{\sqrt{2}} \right)^{c(l)} \prod_{y \in l} \frac{1}{M(y)} \right)^2. \quad (10)$$

The sum now runs over the set \mathcal{L}_{sa} of self-avoiding, closed, non back-tracking loops. Self-avoiding means that the loops may neither self-intersect nor touch each other, they can, however, consist of several disconnected pieces. The loops in \mathcal{L}_{sa} are not oriented, i.e. each loop is counted only with one of its two possible orientations. $c(l)$ again denotes the number of corners of l and the product in (10) runs over all sites y visited by the loops.

Finding a general proof which directly shows the equivalence of the right hand side of (9) at $U_\mu(x) = 1$ with the right hand side of (10) turns out to be a rather hard combinatorial problem. Instead we here discuss an example which illustrates how the two representations are related. The main difference is that the representation (9) for the determinant where also a gauge field is coupled has to work with oriented loops, since the link variables allow to distinguish between forward and backward hopping (complex conjugation in the kernel (1)). Loops in the determinant for a scalar background field give the same contribution when their orientation is reverted, and thus it is possible to find the representation (10) in terms of non-oriented loops.

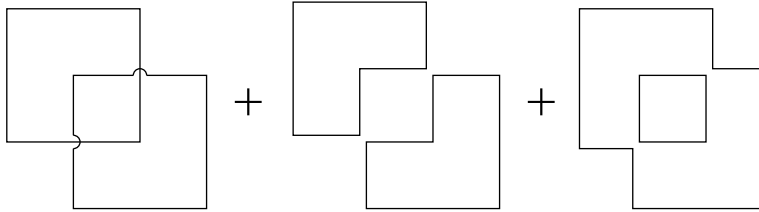


Figure 10: *The contributions to a given configuration as they appear in the scalar formula (10).*

Let's now look at a simple configuration which we depict in Fig. 10. In the figure we show how this term is generated in formula (10), i.e. how it can be written as the product of two self-avoiding loops. There are three ways of doing so, each of them is a cross term in the square, such that we collect an overall factor of 2. The first term gives rise to 8 corners, while the other two configurations each have a total of 12 corners. We thus find a

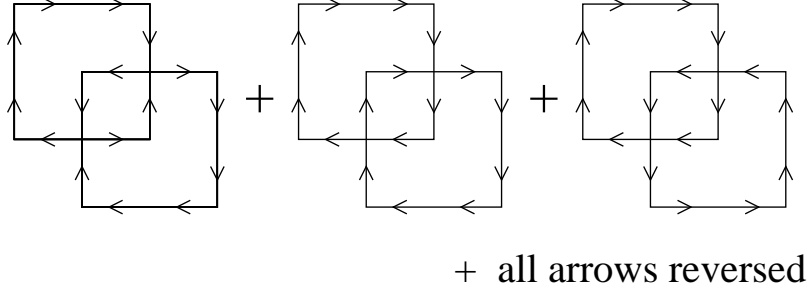


Figure 11: The same contribution as in Fig. 10, now being built from the oriented loops of formula (9).

factor of (the products of $1/M(y)$ are irrelevant here and we suppress them)

$$2 \left[\left(\frac{1}{\sqrt{2}} \right)^8 + \left(\frac{1}{\sqrt{2}} \right)^{12} + \left(\frac{1}{\sqrt{2}} \right)^{12} \right] = \frac{3}{16}.$$

Next we generate the same term, now using the tiling formula (9). Again we find 3 topologically different configurations which we show in Fig. 11. In addition these three configurations come in pairs related to the plotted terms by reverting all arrows. This gives again an overall factor of 2. By collecting the factors for the vertices as given in Fig. 9 we find

$$2 \left[\left(\frac{1}{\sqrt{2}} \right)^8 \times 1 \times 1 + \left(\frac{1}{\sqrt{2}} \right)^8 \times \frac{1}{2} \times \frac{1}{2} + \left(\frac{1}{\sqrt{2}} \right)^8 \times \frac{1}{2} \times \frac{1}{2} \right] = \frac{3}{16}.$$

Thus both formulas (9) and (10) give the same factor. Similarly one can show the equivalence of (9) and (10) for more complicated examples.

Let's now proceed to the case of the strongly coupled Schwinger model. All scalar field variables are set to zero, $\theta(x) = 0$, and we write the U(1) link variables now explicitly as

$$U_\mu(x) = e^{iA_\mu(x)} \quad , \quad A_\mu(x) \in (-\pi, +\pi] .$$

The partition function of the lattice Schwinger model is then given by

$$Z_g = \int_{-\pi}^{\pi} \prod_{(x,\mu)} \frac{dA_\mu(x)}{2\pi} e^{-\frac{1}{g^2} S_{gauge}[A]} \det K . \quad (11)$$

At strong (= infinite) coupling g , the Boltzmann factor for the gauge field equals 1. Only the determinant appears in the integrand. Each t in the sum

over all tilings \mathcal{T} gives rise to links being empty, singly occupied links and doubly occupied links with link variables complex conjugate to each other. These cases correspond to the integrals

$$\int_{-\pi}^{\pi} \frac{dA_{\mu}(x)}{2\pi} = 1, \quad \int_{-\pi}^{\pi} \frac{dA_{\mu}(x)}{2\pi} e^{\pm iA_{\mu}(x)} = 0, \quad \int_{-\pi}^{\pi} \frac{dA_{\mu}(x)}{2\pi} e^{+iA_{\mu}(x)-iA_{\mu}(x)} = 1.$$

The second integral implies that whenever a configuration of tiles contains a link which is occupied only once, the whole configuration vanishes when integrating the gauge field. Thus only configurations with either empty or doubly occupied links (with opposite orientation) contribute in the sum over all tilings, i.e. only the tiles 43, ..., 49 in Fig. 9 contribute. The strong coupling limit thus reduces the lattice Schwinger model to a seven vertex model with vertices and weights as depicted in Fig. 12, where we have included the overall factor $\prod_x (2+m)^2$ into the monomer weight w_1 . Note that after integrating the gauge fields in the strong coupling limit the orientation of the link variables gets lost. Our loops do no longer have an orientation and it is sufficient to have single lines on the tiles in Fig. 12.

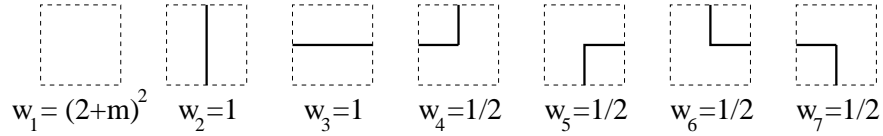


Figure 12: *The 7 vertices occurring in the strong coupling limit and their weights.*

The partition function in the strong coupling limit reads

$$Z_{g=\infty} = \sum_{t \in \mathcal{T}_7} \prod_{j=1}^7 (w_j)^{n_j(t)}. \quad (12)$$

Here \mathcal{T}_7 denotes the set of admissible tilings obtained from the seven tiles depicted in Fig. 12. Formula (12) is equivalent to the partition function for self-avoiding loops with corner activity $1/2$ and monomer weight $(2+m)^2$. The representation (12) for the strongly coupled Schwinger model was first found by Salmhofer [6]. Since [6] uses different techniques (expansion of the Boltzmann factor and local saturation of the Grassmann integral) the derivation of this result as a limiting case of our general formula provides a second non-trivial test of Eq. (9).

It is interesting to note that our representation (9) allows to generalize the vertex model representation for the strongly coupled case to a model with N flavors. For N flavors the integration of the fermions gives the N -th power of the fermion determinant. This simply corresponds to superimposing N different 49-vertex models with loops in N different colors onto each other. Integrating the gauge fields in the strong coupling limit discards all vertices where at least one link is only singly occupied. For the case of the strongly coupled two-flavor Schwinger model this leads to a 163-vertex model [26].

We remark that the representation of the strongly coupled lattice Schwinger model as a seven vertex model demonstrates the power of loop representations when performing numerical simulations. The model (12) has been studied numerically in [27, 28] and high precision data on the phase diagram has been obtained. For vertex models furthermore the use of cluster algorithms might become possible which could further increase the quality of numerical data [29].

5 Integrating out the gauge fields at arbitrary coupling

We now integrate the gauge fields at arbitrary coupling for the model with open boundary conditions. The basic idea is to fill the loops with plaquette variables. We remark that when choosing our lattice to be the above discussed cylinder we find topologically non-trivial loops. For these loops the gauge field integral, although still solvable in closed form, is more involved and for convenience we here discuss only the case of a rectangular lattice with open boundary conditions.

We now assign plaquette variables $V(p)$ to each plaquette p , which are given by the product of the 4 link variables associated to the plaquette p when running through it in mathematically positive direction,

$$V(p) = \prod_{(x,\mu) \in p} U_\mu(x) . \quad (13)$$

To each plaquette p we furthermore assign an occupation number J_p which gives the power of $V(p)$ for the plaquette p . Negative J_p is used when we assign the complex conjugate plaquette variable $V(p)^*$ with exponent $|J_p|$. When two neighboring plaquettes have the same occupation numbers, the link variable shared by the two plaquettes cancels. When the occupation

For a given configuration of occupation numbers J_p the gauge field integral reads,

In our two-dimensional model this integral can easily be solved by choosing a simple gauge, i.e. a maximal tree of link variables set to 1, which factorizes the gauge field integral. The gauge field integral is simply a product over all plaquettes with the factors determined by the occupation numbers,

where the function $F_g(n)$, $n \in \mathbb{Z}$ is given by (we quote the results for Wilson action as well as for Villain action),

22

Here I_n denotes the modified Bessel function. For the partition function of the lattice Schwinger model we thus find,

$$Z_g = \int \prod_{(x,\mu)} dU_\mu(x) e^{-\frac{1}{g^2} S_{gauge}} \det K = \sum_{t \in \mathcal{T}} \prod_{j=1}^{49} (\tilde{w}_j)^{n_j(t)} \prod_p F_g(J_p(t)) . \quad (17)$$

The last term denotes the product over all plaquette factors depending on the occupation numbers $J_p(t)$ for a given tiling t . We remark that we now have included the factors of $(2+m)$ into the new weights \tilde{w}_j . They are obtained by multiplying the old weight w_{43} by $(2+m)^2$, by multiplying weights w_1, \dots, w_{12} with $2+m$ and setting $\tilde{w}_j = w_j$ for the remaining weights.

Our expression (17) represents the partition function as a sum over discrete variables. This expression could lead to the possibility of applying cluster algorithms [29] which might considerably improve the quality of numerical data.

6 Observables

In this section we discuss the loop representations for pure gauge field observables such as the Wilson loop and for local fermionic observables in particular scalars and vectors.

Let's start with the simpler observables which are the ones only containing gauge fields. The prototype of such an observable is the Wilson loop

$$W_{\mathcal{C}}(U) = \prod_{(x,\mu) \in \mathcal{C}} U_\mu(x) .$$

Here \mathcal{C} is a closed contour and without restriction of generality we assume that it is oriented in mathematically positive direction. As for the fermion loops, we can create the link variables on \mathcal{C} by filling the whole contour with plaquette variables as defined in (13). This requires an occupation number of +1 for all plaquettes inside \mathcal{C} . This occupation number can simply be added to the occupation numbers J_p from the fermion loops. When integrating out the gauge fields we find for the vacuum expectation value of the Wilson loop in the lattice Schwinger model (compare (17))

$$\langle W_{\mathcal{C}}(U) \rangle_g = \frac{1}{Z_g} \sum_{t \in \mathcal{T}} \prod_{j=1}^{49} (\tilde{w}_j)^{n_j(t)} \prod_p F_g(J_p(t) + \chi_p(\mathcal{C})) , \quad (18)$$

where we defined $\chi_p(\mathcal{C})$ to be the characteristic function of the area inside the chosen contour \mathcal{C} with $\chi_p(\mathcal{C}) = 1$ for plaquettes p in the interior of \mathcal{C} and $\chi_p(\mathcal{C}) = 0$ for plaquettes outside. It is obvious that this formula can easily be generalized to more involved gauge invariant observables for the gauge field.

Only slightly more complicated is the loop representation for local fermionic observables, in particular scalars and vectors. Here we can make use of the fact, that our formalism gives the fermion determinant, i.e. the fermionic path integral, in an arbitrary gauge field and in an arbitrary local scalar field $\theta(x)$. Thus by differentiating the determinant with respect to these external fields we can generate n-point functions for the fermionic bilinears in the action, i.e. scalars and vectors. By writing the link variables as $U_\mu(x) = \exp(iA_\mu(x))$ with $A_{-\mu}(x) = -A_\mu(x - \hat{\mu})$, the kernel K for the fermion action reads (compare (1))

$$K(x, y) = \left[2 + m + \theta(x) \right] \delta_{x, y} - \sum_{\mu=\pm 1}^{\pm 2} \frac{1 \mp \sigma_\mu}{2} e^{iA_\mu(x)} \delta_{x+\hat{\mu}, y} .$$

Thus we obtain for the expectation value (just the fermion integration) of scalars and vectors

$$\begin{aligned} & \left\langle \prod_{k=1}^M \bar{\psi}\psi(v_k) \prod_{l=1}^N j_{\nu_l}(z_l) \right\rangle_{fermions} \\ &= \int d\bar{\psi} d\psi e^{-\sum_{x,y} \bar{\psi}(x) K(x,y) \psi(y)} \prod_{k=1}^M \bar{\psi}\psi(v_k) \prod_{l=1}^N j_{\nu_l}(z_l) \\ &= (-1)^M \prod_{k=1}^M \frac{\partial}{\partial \theta(v_k)} (i)^N \prod_{l=1}^N \frac{\partial}{\partial A_{\nu_l}(z_l)} \int d\bar{\psi} d\psi e^{-\sum_{x,y} \bar{\psi}(x) K(x,y) \psi(y)} \\ &= (-1)^M \prod_{k=1}^M \frac{\partial}{\partial \theta(v_k)} (i)^N \prod_{l=1}^N \frac{\partial}{\partial A_{\nu_l}(z_l)} \det K . \end{aligned}$$

The current $j_\nu(z)$ is the Noether current corresponding to the gauge symmetry of our action

$$\begin{aligned} j_\nu(z) &= \frac{1}{2} \left[\bar{\psi}(z) \sigma_\nu U_\nu(z) \psi(z + \hat{\nu}) + \bar{\psi}(z + \hat{\nu}) \sigma_\nu U_\nu(z)^* \psi(z) \right] \\ &- \frac{1}{2} \left[\bar{\psi}(z) U_\nu(z) \psi(z + \hat{\nu}) - \bar{\psi}(z + \hat{\nu}) U_\nu(z)^* \psi(z) \right] . \end{aligned} \quad (19)$$

In the continuum limit the first term turns into the vector-current $\bar{\psi}(z)\gamma_\nu\psi(z)$ while the second term is of order $\mathcal{O}(a)$ and vanishes.

Now we act with the differential operators $\partial/\partial\theta(v)$ and $\partial/\partial A_\nu(z)$ on our loop expression (9). When making explicit all external fields the formula (9) reads (now again using the original vertex weights w_i from Fig. 9 and not the rescaled vertices \tilde{w}_i used in (17))

$$\det K = \prod_{x \in \Lambda} [2 + m + \theta(x)]^2 \sum_{t \in \mathcal{T}} \prod_{j=1}^{49} (w_j)^{n_j(t)} \prod_{(y, \mu) \in t} \frac{e^{\pm i A_\mu(y)}}{2 + m + \theta(y)}. \quad (20)$$

In the numerator of the last term which collects the link factors, the plus sign in the exponent has to be taken for links (y, μ) which are run through in positive direction for the configuration t and the minus sign is taken for links occupied in negative direction. When acting with $\partial/\partial\theta(v)$ for some fixed site v on the expression (20) we have to distinguish three different cases. When two fermion lines run through v , all terms containing $\theta(v)$ cancel each other and the differentiation simply gives zero. When one fermion line runs through v this contribution is linear in $2 + m + \theta(v)$ and after differentiation there remains a factor of 1. Finally when the site v is empty the factor in (20) is $[2 + m + \theta(v)]^2$ and the action of the differential operator then gives a weight of $2[2 + m + \theta(v)]$. The results for these three cases can be denoted conveniently by inserting the following factor in the sum over the configurations $t \in \mathcal{T}$ (we have now set the scalar field θ to zero everywhere which gives us the expression for the Schwinger model)

$$\left[1 - S_v^{(2)}(t)\right] \left(\frac{1}{2 + m}\right)^{S_v^{(1)}(t)} \left(\frac{2}{2 + m}\right)^{S_v^{(0)}(t)}, \quad (21)$$

where we defined $S_v^{(n)}(t)$ to be equal to 1 when the site v is visited exactly n -times by the fermion loops of the configuration t and zero otherwise. The first factor in (21) produces a zero whenever 2 fermion lines run through v . The other two terms correct the weight at v for the cases of a single fermion line and for v being empty.

The result for the differential operator $i\partial/\partial A_\nu(z)$ is even simpler to denote. From (20) it is clear that for configurations t where the link (z, ν) is empty, or configurations where this link is doubly occupied and the link variables cancel each other due to their opposite orientation, this contribution does not depend on $A_\nu(z)$ and is annihilated by $i\partial/\partial A_\nu(z)$. For configurations where the link (z, ν) is run through with positive orientation,

we obtain after applying $i\partial/\partial A_\nu(z)$ a factor of -1 and a factor of $+1$ for negative orientation. Thus the differential operator simply measures the negative of the net flow of fermion lines through the link (z, ν) . By defining

$$L_{(z,\nu)}(t) = \begin{cases} +1 & \text{when } t \text{ occupies } (z, \nu) \text{ in positive direction} \\ -1 & \text{when } t \text{ occupies } (z, \nu) \text{ in negative direction} \\ 0 & \text{when } t \text{ has net flux zero through } (z, \nu) \end{cases}, \quad (22)$$

we can take into account the vectors by simply including $-L_{(z,\nu)}(t)$ in the sum. Inserting this factor, together with (21) into the sum over all configurations we obtain for the fermionic n-point functions in the lattice Schwinger model (the gauge fields were integrated out as above, $\theta(x)$ is set to 0, and we use again the rescaled weights \tilde{w}_i as defined below equation (17))

$$\begin{aligned} \left\langle \prod_{k=1}^M \bar{\psi}\psi(v_k) \prod_{l=1}^N j_{\nu_l}(z_l) \right\rangle_g &= (-1)^{M+N} \frac{1}{Z_g} \sum_{t \in \mathcal{T}} \prod_{j=1}^{49} (\tilde{w}_j)^{n_j(t)} \prod_p F_g(J_p(t)) \\ &\times \prod_{k=1}^M \left[[1 - S_{v_k}^{(2)}(t)] \left(\frac{1}{2+m} \right)^{S_{v_k}^{(1)}(t)} \left(\frac{2}{2+m} \right)^{S_{v_k}^{(0)}(t)} \right] \prod_{l=1}^N L_{(z_l, \nu_l)}(t). \end{aligned} \quad (23)$$

After getting used to it, this expression turns out to be very powerful and also very simple from a numerical point of view. For computing n-point functions of scalars one merely has to locally change the weights on the sites supporting the scalars, and for vectors only the net flux through the links associated with the currents has to be counted. This is certainly much simpler than inverting the fermion matrix as is necessary in the standard numerical approach.

It is instructive to play a little bit with formula (23), so let's e.g. show that $\langle j_\nu(z) \rangle_g = 0$. As discussed above only configurations where the link (z, ν) is singly occupied can contribute. These configurations, however, come in pairs related by reversing the orientation of all fermion lines. The two contributions have the same weight from the gauge fields ($J_p \rightarrow -J_p$) but are counted with opposite sign in (23) and thus the one-point function of the current vanishes as it should.

Furthermore it is interesting to analyze some variables in the strong coupling limit, in particular the chiral condensate $\langle \bar{\psi}\psi(v) \rangle_{g=\infty}$. As discussed above, in the strong coupling limit all configurations with singly occupied links are suppressed. Thus, according to (21), the chiral condensate can obtain contributions only from the empty vertex. Using translational in-

variance of $\langle \bar{\psi}\psi(v) \rangle_{g=\infty}$ on the infinite lattice, one finds (compare Eq. 12)

$$\langle \bar{\psi}\psi(v) \rangle_{g=\infty} = \frac{2}{2+m} \lim_{\Lambda \rightarrow \infty} \frac{1}{Z_{g=\infty}} \sum_{t \in \mathcal{T}_7} \prod_{j=1}^7 (w_j)^{n_j(t)} \frac{n_1(t)}{|\Lambda|}. \quad (24)$$

Thus in the strong coupling limit the chiral condensate is proportional to the density of vertex 1 of Fig. 12, i.e. the empty tile. Similarly it is possible to obtain simple expressions for other fermionic observables in the strong coupling limit.

7 Discussion

In this article we have derived the loop representation for the fermion determinant of 2-D Wilson lattice fermions coupled to U(1) gauge fields, i.e. the fermion determinant of the lattice Schwinger model. The construction is based on first using standard hopping expansion which already expresses the determinant in terms of loops which are the natural (gauge invariant) variables for the fermion determinant. Standard hopping expansion, however, only gives a loop expansion for the free energy, and thus to obtain the desired result, the Boltzmann factor was expanded. An essential ingredient for this expansion was the introduction of a locally varying mass term. For our problem it was shown that the determinant is a polynomial in the local mass terms with a degree of two. This considerably restricts the number of terms which can appear when expanding the Boltzmann factor. For the remaining terms it was shown that they can be obtained by summing over local pieces of loops, i.e. over the vertices given in Fig. 9.

The gauge fields were integrated out and the result was expressed in terms of occupation numbers for the plaquettes enclosed in the fermion loops. The whole formalism generalizes to the case of non-vanishing chemical potential in a natural way. Gauge field variables can be treated on the same footing as the fermion loops, i.e. by assigning occupation numbers for the plaquettes followed by integrating the link variables. Local fermionic observables were generated by differentiating the determinant with respect to the external fields. In the loop picture their vacuum expectation values simply correspond to counting the net flow of fermion loops through the sites (for scalars) and links (vectors) of the lattice.

Certainly the lattice Schwinger model is a relatively simple system, but the essential ingredients of our construction can be carried over to more

realistic models. In particular, a hopping expansion of the fermion determinant for Wilson fermions is straightforward also for higher dimensions and non-abelian gauge groups. Furthermore the necessary traces over the γ -matrices can be computed in closed form also in 4 dimensions [17]. It is also possible to again apply the trick of introducing a locally varying mass term and, in the region of convergence, use it to rule out infinitely many terms in the expansion of the Boltzmann factor. The number of allowed loops running through links and sites will depend on the dimension of the problem and the number of colors. We expect that also in higher dimensions it is possible to decompose the loops into local elements. For non-abelian models, these elements will, however, be more involved, since also for the gauge fields one now has to compute traces. The inclusion of chemical potential can be treated in exactly the same way as we have done for the Schwinger model. Also local fermionic observables will again correspond to counting the net flow of fermion lines through sites and links. The treatment of the gauge field integral, however, becomes more complicated. For abelian fields in higher dimensions it is still possible to build the links on our loops by filling surfaces [5], and a subsequent duality transformation (see e.g. [30]) produces simple Gaussian weights. For non-abelian gauge groups no such techniques are known and probably one would have to rely on perturbative calculations.

We remark that also fermionic models such as the Thirring model or the Gross-Neveu model are accessible to the techniques developed here. The four-fermi terms are then generated by coupling an auxiliary field to fermionic bilinears and these auxiliary fields are subsequently integrated with Gaussian measures. The auxiliary fields necessary for generating the above mentioned models are abelian fields and also their Gaussian integrals are straightforward to solve (see e.g. [10] for a study of this approach to the Gross-Neveu model in 2D). Thus for purely fermionic models the tools for finding a loop representation are readily available. It is hoped that such a representation opens new ways for numerical simulations of these systems, in particular for the case of non-vanishing chemical potential.

Acknowledgement: I have considerably profited from discussions with Mark Alford and Uwe-Jens Wiese. My special thanks goes to Christian Lang who in addition to valuable comments also provided me with the results of his computer-algebraic evaluation of the fermion determinant on small lattices.

References

- [1] P. Rossi and U. Wolff, Nucl. Phys. B248 (1984) 105.
- [2] M. Karowski, R. Schrader and H.J. Thun, Commun. Math. Phys. 97 (1985) 5.
- [3] I. Montvay, Phys. Lett. B227 (1989) 260.
- [4] I. Montvay, in: *Probabilistic Methods in Quantum Field Theory*, P.H. Damgaard et al. (Eds.) Plenum Press, New York 1990.
- [5] J.M. Aroca, H. Fort and R. Gambini, Phys. Rev. D57 (1998) 3701; H. Fort, *The worldsheet formulation as an alternative method for simulating dynamical fermions*, Report hep-lat/9710082; Nucl. Phys. Proc. Suppl. 63 (1998), 793.
- [6] M. Salmhofer, Nucl. Phys. B362 (1991) 641.
- [7] K. Scharnhorst, Nucl. Phys. B479 (1996) 727.
- [8] K. Scharnhorst, Nucl. Phys. B503 (1997) 479.
- [9] C. Gatttringer, *A formula for the hopping expansion of 8-vertex models coupled to an external field*, Int. J. Mod. Phys. A (in print), Report cond-mat/9811139.
- [10] C. Gatttringer, Nucl. Phys. B543 (1999) 533.
- [11] M. Creutz, Phys. Rev. Lett. 81 (1998) 3555.
- [12] S. Chandrasekharan and U.-J. Wiese, Report cond-mat/9902128.
- [13] I. Montvay and G. Münster, *Quantum Fields on a Lattice*, Cambridge University Press, Cambridge 1994.
- [14] X.Q. Luo, Z. Phys. C48 (1990) 283.
- [15] M. Reed and B. Simon, *Methods of Modern Mathematical Physics, Vol. IV: Analysis of Operators*, Academic Press, New York 1978.
- [16] D.H. Weingarten and J.L. Challifour, Ann. Phys. 123 (1979) 61.
- [17] I.O. Stamatescu, Phys. Rev. D25 (1981) 1130.

- [18] C.R. Gattringer, S. Jaimungal and G.W. Semenoff, *Loops, surfaces and Grassmann Representation for Two- and Three-Dimensional Ising Models*, Report hep-th/9801098, to appear in Int. J. of Mod. Phys. A.; C. Gattringer, Nucl. Phys. B (Proc. Suppl.) 73 (1999) 772.
- [19] H. Heuser, *Lehrbuch der Analysis, Vol. I*, Teubner, Stuttgart 1984.
- [20] C. Fan and F.Y. Wu, Phys. Rev. 179 (1969) 179.
- [21] C. Fan and F.Y. Wu, Phys. Rev. B2 (1970) 723.
- [22] R. Baxter, *Exactly Solved Models in Statistical Mechanics*, Academic Press, London 1982.
- [23] C. Gattringer, H. Gausterer and J. Steiner, work in preparation.
- [24] R.F. Alvarez-Estrada and A.G. Nicola, Phys. Rev. D57 (1998) 3618.
- [25] P. Hasenfratz and F. Karsch, Phys. Lett. B125 (1983) 308.
- [26] C.B. Lang, private communication.
- [27] H. Gausterer, C.B. Lang and M. Salmhofer, Nucl. Phys. B388 (1992) 275; H. Gausterer and C.B. Lang, Nucl. Phys. B455 (1995) 785.
- [28] F. Karsch, E. Meggiolaro and L. Turko, Phys. Rev. D51 (1995) 6417.
- [29] H.G. Evertz, G. Lana and M. Marcu, Phys. Rev. Lett. 70 (1993) 875; U.-J. Wiese, Phys. Lett. B311 (1993) 235.
- [30] R. Savit, Rev. Mod. Phys. 52 (1980) 453.